Ref.TH.2285-CERN

ASYMPTOTIC FREEDOM EFFECTS IN ν AND $\bar{\nu}$ DEEP INELASTIC SCATTERING

A.J. Buras

CERN -- Geneva

A B S T R A C T

We present an analysis of the effects of asymptotic freedom on charged current ν and $\bar{\nu}$ deep inelastic scattering. We consider both the GIM model and the five-quark model with right-handed couplings. We calculate the Q^2 dependence of the quark distributions as given by asymptotic freedom, and we use these distributions to calculate $\sigma^{\bar{\nu}}/\sigma^{\nu}$, $\langle y \rangle_{\bar{\nu}}$ as well as x and y distributions. We study the effects of asymptotic freedom in charm and b quark production. We also discuss the sensitivity of our results to the shape of the gluon distribution. We emphasize the importance of comparing theory with data excluding low Q^2 values (say $Q^2 \geq 2$ GeV^2) in attempting to resolve the high y anomaly controversy.

Ref.TH.2285-CERN

1 March 1977

1. - INTRODUCTION

Recently [1)-11)] there has been an increased interest in the application of asymptotically free gauge theories [12),13)] (hereafter ASFT) to the deep inelastic data. This increased interest is due to the observation of scaling violations [14)-17)] in both electroproduction and charged current neutrino (antineutrino) scattering. Since scaling violations emerge rather naturally in the theories in question it is of great importance to check whether these theories account for the deviations from scaling observed in the data.

Apparently the situation is not the same in neutrino and electroproduction processes. Whereas many theorists agree that the pattern of scaling violations observed in the electroproduction data is in good agreement with ASFT predictions, there is a controversy concerning neutrino (antineutrino data). On the one hand there is a fraction of physicists [2),5)] claiming that ASFT can explain so-called high y anomalies. On the other hand many theorists attribute [3),6),7)] the anomalies in question to the manifestation of new quarks with right-handed weak couplings [18)], ASFT effects being found too small to explain the data.

This controversy stems not only from the relatively poor data, but also from various assumptions and approximations which plague analyses of this type.

One of the approximations used by various authors is the following. The theory gives predictions only for the moments of suitably chosen structure functions as Q^2 is varied, whereas the neutrino (antineutrino) data are given as functions of the incoming energy $E_\nu (E_{\bar\nu})$. The "technique" to circumvent this difficulty employed by some authors [2),7)] is to evaluate the moments at an energy dependent effective Q^2_{eff} value and to obtain in this way the energy dependence of the relevant quantities. This method, although interesting and apparently relatively accurate can be criticized as follows *). Since this technique gives the moments at fixed finite energy, to be consistent the integration over x from 0 to 1 should correspond to the integration over Q^2 from 0 to 2ME. This task is impossible to do since the perturbative calculations on which the results of ASFT are based are unreliable for $Q^2 \leq O(1)$ GeV^2, the effective coupling being too large in this range of Q^2.

---

*) For related criticisms, see Refs. 3), 6), 19).

Another method employed by some authors [3] is to factorize the x and Q^2 dependence of the structure functions and take the latter dependence as given by ASFT. Although this method is probably suitable for obtaining upper bounds on scaling violations predicted by ASFT for total cross-sections and $\langle y \rangle$, it is unacceptable for the calculation of x distributions since one of the spectacular features of ASFT, as well as of all renormalizable field theories, is the absence of factorization in x and Q^2.

We think that the only consistent method within the given approximations (neglect of higher twist contributions, higher order corrections in the gluon coupling, etc.) is to invert the moments (which implies assuming certain uniformity properties) and use the structure functions (parton distributions) obtained to calculate the deep inelastic scattering, keeping the cut-off $Q^2 \geq Q_0^2$. Correspondingly, we think that field theorists should ask their experimental friends to cut their data at some Q_0^2, above which the coupling is sufficiently small and that perturbative calculations make sense. Otherwise one is forced to make assumptions about $Q^2 \leq Q_0^2$ region, about which present field theory has little to say. At $E_\nu = 30$ GeV and $Q_0^2 = 2$ GeV^2 this corresponds to making assumptions (outside the field theoretical framework) on the behaviour of about 40% of the cross-section. This is certainly not the best way to test field theory.

In this paper we shall proceed as follows. We shall first find the Q^2 dependence of the quark distributions as given by ASFT *). Having Q^2 dependent quark densities at hand we shall calculate (keeping the cut-off $Q^2 \geq 2$ GeV^2) $\sigma_{\bar{\nu}}/\sigma_\nu$ and $\langle y \rangle_{\bar{\nu}}$ as well as various properties of x and y distributions as functions of E_ν ($E_{\bar{\nu}}$). To our knowledge, the ASFT calculations as presented in the literature so far have been limited to global quantities such as $\langle y \rangle_{\bar{\nu}}$ and $\sigma_{\bar{\nu}}/\sigma_\nu$ **). The hope is that x and y distributions may also be useful in distinguishing between various models once better data are available.

We shall also make estimates of the cross-sections for charm and bottom production within ASFT framework and compare them with simple parton model results.

---

*) Q^2 dependent quark distributions have been recently discussed in Refs. 5), 20).

**) A qualitative discussion of x and y distributions within ASFT has been given in Ref. 21).

Since data are usually presented without the proper cut-off in Q^2 we shall also show the results of calculations in which we have made certain assumptions about the $Q^2 \leq 2\ GeV^2$ region. As we already stressed we do not have confidence in such a procedure, nevertheless we show these results for illustration and comparison with Q^2 cut results.

There is still another point to be stressed. In order to obtain Q^2 dependence of parton densities within ASFT one has to make assumptions about the distributions of quarks and gluons at a particular value of Q^2 (see Section 2 for details). Although there exists a reasonable knowledge of the distributions of valence quarks and some knowledge about the sea, little is known about the corresponding distributions for gluons. So it is of importance to investigate how various results depend on the assumed gluon distribution. A progress in this direction has been made in Refs. 1) and 22) where the dependence in question has been calculated for electroproduction structure functions and Drell-Yan cross-sections, respectively. Here we shall investigate how the assumptions on the gluon distribution affect the calculations of neutrino and antineutrino cross-sections.

Our paper is organized as follows. In Section 2 we recall those formulae of ASFT which we have used to calculate the Q^2 dependence of the quark distributions. We present these formulae in a form useful for phenomenological applications. In Section 3 we discuss the Q^2 dependence of the parton distributions for various choices of the gluon distribution. In Section 4 we present the ASFT calculations of neutrino (antineutrino) cross-sections and distributions in the framework of the GIM model and the b quark model [22] with right-handed couplings. Finally, in Section 5 we briefly summarize our results and comment on the effects which we have neglected in our analysis.

2. - BASIC FORMULAE OF ASFT

In this section we shall recall those formulae of asymptotically free gauge theory which we have used in the phenomenological applications. It will be convenient to work with Q^2 dependent quark and gluon distributions.

Following Ref. 2) we decompose parton distributions into valence, sea and charm contributions according to

$$\begin{aligned} p(x,Q^2) &= p_v(x,Q^2) + s(x,Q^2) \\ n(x,Q^2) &= n_v(x,Q^2) + s(x,Q^2) \\ \bar{n}(x,Q^2) &= \bar{p}(x,Q^2) = \lambda(x,Q^2) = \bar{\lambda}(x,Q^2) \equiv s(x,Q^2) \\ p'(x,Q^2) &= \bar{p}'(x,Q^2) \equiv c(x,Q^2) \end{aligned} \tag{2.1}$$

and introduce a gluon distribution $G(x,Q^2)$.

We denote the moments of the quark and gluon distributions by

$$\langle q(Q^2)\rangle_n \equiv \int_0^1 dx\, x^{n-1} q(x,Q^2)$$

and

$$\langle G(Q^2)\rangle_n \equiv \int_0^1 dx\, x^{n-1} G(x,Q^2) \qquad n \geq 2 \tag{2.2}$$

respectively.

Restricting considerations to isoscalar targets we are left with the following combinations of quark distributions

$$\begin{aligned} V(x,Q^2) &\equiv p_v(x,Q^2) + n_v(x,Q^2) \\ \tilde{V}(x,Q^2) &\equiv V(x,Q^2) + S(x,Q^2) - 3C(x,Q^2) \\ q^S(x,Q^2) &\equiv V(x,Q^2) + S(x,Q^2) + C(x,Q^2) \end{aligned} \tag{2.3}$$

Here

$$S(x, Q^2) \equiv 6\, s(x, Q^2)$$

and

$$C(x, Q^2) \equiv 2\, c(x, Q^2) \tag{2.4}$$

V and $\tilde{V}$ transform as non-singlets (λ_8 and λ_{15}) and q^s as a singlet under the physical SU(4).

The Q^2 dependence of $V(x,Q^2)$, $S(x,Q^2)$, $C(x,Q^2)$ and $G(x,Q^2)$ as given in ASFT is obtained by solving the following set of equations *)

$$\langle V(Q^2)\rangle_n = \langle V(Q_0^2)\rangle_n \exp\left[-\gamma_{\psi\psi}^n s\right], \tag{2.5}$$

$$\langle \tilde{V}(Q^2)\rangle_n = \langle \tilde{V}(Q_0^2)\rangle_n \exp\left[-\gamma_{\psi\psi}^n s\right], \tag{2.6}$$

$$\begin{aligned}\langle q^s(Q^2)\rangle_n = &\left\{(1-\alpha_n)\langle q^s(Q_0^2)\rangle_n - \beta_n \langle G(Q_0^2)\rangle_n\right\} \exp\left[-\gamma_+^n s\right] \\ &+ \left\{\alpha_n \langle q^s(Q_0^2)\rangle_n + \beta_n \langle G(Q_0^2)\rangle_n\right\} \exp\left[-\gamma_-^n s\right]\end{aligned} \tag{2.7}$$

and

$$\begin{aligned}\langle G(Q^2)\rangle_n = &\left\{\alpha_n \langle G(Q_0^2)\rangle_n - \varepsilon_n \langle q^s(Q_0^2)\rangle_n\right\} \exp\left[-\gamma_+^n s\right] \\ &+ \left\{(1-\alpha_n)\langle G(Q_0^2)\rangle_n + \varepsilon_n \langle q^s(Q_0^2)\rangle_n\right\} \exp\left[-\gamma_-^n s\right]\end{aligned} \tag{2.8}$$

---

*) Equations (2.7) and (2.8) can be derived from the results of Ref. 13) by diagonalizing the renormalization group equations.

The various quantities appearing in (2.5)-(2.8) are given in an SU(3) gauge theory by *)

$$\gamma_{\pm}^{n} = \frac{\gamma_{\psi\psi}^{n} + \gamma_{AA}^{n} \pm \sqrt{(\gamma_{\psi\psi}^{n} - \gamma_{AA}^{n})^2 + 4\gamma_{\psi A}^{n}\gamma_{A\psi}^{n}}}{2} \tag{2.9}$$

where

$$\begin{aligned}
2b\,\gamma_{\psi\psi}^{n} &= \frac{8}{3}\left[1 - \frac{2}{n(n+1)} + 4\sum_{J=2}^{n}\frac{1}{J}\right], \\
2b\,\gamma_{AA}^{n} &= 6\left[\frac{1}{3} - \frac{4}{n(n-1)} - \frac{4}{(n+1)(n+2)} + 4\sum_{J=2}^{n}\frac{1}{J}\right] + \frac{4}{3}m, \\
2b\,\gamma_{\psi A}^{n} &= m\left[\frac{8}{n+2} + \frac{16}{n(n+1)(n+2)}\right], \qquad n \geq 2 \\
2b\,\gamma_{A\psi}^{n} &= \frac{8}{3}\left[\frac{1}{n+1} + \frac{2}{n(n-1)}\right].
\end{aligned} \tag{2.10}$$

Here $b = \frac{1}{3}(33-2m)$ with m being the number of flavours. In this paper we take $m = 4$.

The α_n, β_n and ϵ_n are given by

$$\alpha_n = \frac{\gamma_{\psi A}^{n}\gamma_{A\psi}^{n}}{\gamma_{\psi A}^{n}\gamma_{A\psi}^{n} + [\gamma_{-}^{n} - \gamma_{\psi\psi}^{n}]^2}$$

$$\beta_n = \alpha_n \frac{(\gamma_{\psi\psi}^{n} - \gamma_{-}^{n})}{2\gamma_{A\psi}^{n}} \tag{2.11}$$

and

$$\epsilon_n = \frac{(1-\alpha_n)\alpha_n}{\beta_n}.$$

---

*) We use the notation of Ref. 12).

Furthermore

$$s = \ln\left[\frac{\ln\frac{Q^2}{\Lambda^2}}{\ln\frac{Q_0^2}{\Lambda^2}}\right] \tag{2.12}$$

where Q_0^2 is the reference momentum at which various parton densities will be taken from the data. Λ is the parameter which gives the momentum at which the effective gluon coupling constant

$$\alpha_s(Q^2) \equiv \frac{\bar{g}^2(Q^2)}{4\pi} = \frac{12\pi}{(33-2n)\ln\frac{Q^2}{\Lambda^2}} \tag{2.13}$$

becomes large. The values $0.2 \le \Lambda \le 0.5$ assure [9] that $\alpha_s(Q^2)$ is large for $Q^2 \sim 0.3$ GeV^2, where bound state effects are important, and is small enough for $Q^2 \ge 2$ GeV^2 that perturbative calculations make sense.

In order to solve the equations (2.5)-(2.8) one has to make assumptions about the input moments

$$\langle V(Q_0^2)\rangle_n \,,\ \langle \tilde{V}(Q_0^2)\rangle_n \,,\ \langle q^s(Q_0^2)\rangle_n \quad \text{and} \quad \langle G(Q_0^2)\rangle_n \,.$$

We shall discuss this in the subsequent section.

Since the equations (2.5)-(2.8), although sometimes in a different form, have been already discussed in the literature [2),4),5)] we shall not list their properties, which will anyway be evident from the results of Section 3. Nevertheless, for the convenience of the reader we have presented in Table I the values of β_n, α_n, $\gamma_{\pm}^n$, γ_{AA}^n and $\gamma_{\psi\psi}^n$ for $n = 4$ and $n = 2 \ldots 5$. Notice that $\alpha_2 = \beta_2$ and $\gamma_-^2 = 0$ assure energy-momentum conservation. Also as n increases $\alpha_n \to 1$, $\beta_n \to 0$, $\epsilon_n \to 0$, $\gamma_-^n \to \gamma_{\psi\psi}^n$ and $\gamma_+^n \to \gamma_{AA}^n$ telling us that for higher moments (large n) the Q^2 dependence of quark distributions decouples from that of the gluons

$$\langle q^s(Q^2)\rangle_n \approx \langle q^s(Q_0^2)\rangle_n \exp\left[-s\,\gamma_{\psi\psi}^n\right] \,,$$

$$\langle G(Q^2)\rangle_n \approx \langle G(Q_0^2)\rangle_n \exp\left[-s\,\gamma_{AA}^n\right] \tag{2.14}$$

In technical terms it means that as $n \to \infty$ $(x \to 1)$ the mixing between gluon and quark singlet operators becomes weaker and weaker.

In fact, as shown in Table 1, the mixing in question is only strong for $n = 2$ due to energy-momentum conservation. For $n \neq 2$ it is relatively weak and consequently the Q^2 dependence of the quark distributions is not dramatically dependent on the shape of the gluon distribution, once the momentum carried by gluons at $Q^2 = Q_o^2$ has been fixed.

Having set up the whole apparatus we shall now solve the equations (2.5)-(2.8).

3. - Q^2 DEPENDENCE OF THE QUARK DISTRIBUTIONS

3.1 - Input moments

In order to solve Eqs. (2.5)-(2.8) we have to know the input moments

$$\langle V(Q_o^2)\rangle_n \,, \quad \langle S(Q_o^2)\rangle_n \,, \quad \langle C(Q_o^2)\rangle_n \quad \text{and} \quad \langle G(Q_o^2)\rangle_n \,.$$

In choosing the input values of $< V(Q_o^2) >_n$ and $< S(Q_o^2) >_n$ we have been guided by the parametrizations of Barger and Phillips [23].

Our parametrizations at Q^2, the value to be specified below, are as follows.

i) Valence quarks

$$x V(x, Q_o^2) = 3 \cdot 1.73 \; x^{0.65} (1-x)^3 \tag{3.1}$$

This parametrization gives almost as good fit to the low Q^2 neutrino and electroproduction data as that of Ref. 23), but is simpler. It is certainly a better parametrization of the data than the form $x^{\frac{1}{2}}(1-x)^3$ used by many authors. The normalization factor 3 assures that $\int dx V(x) = 3$, a property often forgotten in the literature.

ii) Non-charmed sea

$$x\,S(x,Q_0^2) = 0.87\,(1-x)^9 \qquad (3.2)$$

This is the parametrization of Ref. 23). This parametrization leads to a value of $\nu W_2(x\approx 0,\ Q^2 = 2\ \mathrm{GeV}^2)$ which is slightly lower than that observed in the electroproduction [16] and μp data [17]. We have checked, however, that for $Q^2 \geq 3.5\ \mathrm{GeV}^2$ this discrepancy is cured by the contribution of the charmed sea.

iii) Charmed sea

Having no information about charmed quarks in the nucleon we assume, following Refs. 2), 7),

$$x\,C(x,Q_0^2) \equiv 0 \qquad (3.3)$$

The equations (2.5)-(2.8) will then develop a non-zero charmed sea for $Q^2 > Q_0^2$.

iv) Gluons

Since the gluon distribution is unknown, we have to consider various choices. Following Refs. 1), 22), we assume

$$x\,G(x,Q_0^2) = 0.493\,(1-x)^{\eta}(1+\eta) \qquad (3.4)$$

with η being a free parameter, which we shall vary. The factor 0.493 comes from momentum conservation.

Having all the parton densities at the reference momentum Q_0^2 we can now calculate the input moments entering Eqs. (2.5)-(2.8) and subsequently obtain xV, xS and xC as functions of x and s. In order to find the Q^2 dependence of the distributions in question we have to specify Q_0^2 and Λ. We have already fixed Λ to be in the range $0.2 \leq \Lambda \leq 0.5$ GeV. In our subsequent applications to deep inelastic scattering we shall use only the value $\Lambda = 0.5$ GeV corresponding to the maximal scaling violations for this range of values of Λ. Since we shall also present the free parton

model results it will be easy to find where approximately the curves corresponding to $\Lambda < 0.5$ should lie. For Q_o^2 we take the value 2 GeV^2. At this value of Q^2 the fits (3.1) and (3.2) are good representations of the neutrino data and the amount of charmed sea is presumably consistent with Eq. (3.3).

Since not everyone may agree with our assumptions about Λ and Q_o^2 we present our results as functions of s rather than of Q^2. We supply, however, the reader with Table II, from which she(he) can read the corresponding values of Q^2 for the limiting choices of Λ.

3.2 - Solution of the ASFT equations

In previous analyses [5),20)] the Q^2 dependence of quark densities as given by ASFT has been given in a numerical form. We think it is useful to have instead analytic expressions which, to a very good accuracy, represent the Q^2 dependence predicted by ASFT. This can be done by choosing certain quark distributions with a few free parameters and determining the latter from Eqs. (2.4)-(2.8).

We present here only the analytic expression for the Q^2 dependence of the valence quark distribution since the corresponding expressions for the sea are very long. We hope to find more elegant expressions in the future. The fact that the Q^2 dependence of the valence quarks is simpler than that of the sea quarks is easy to understand. The valence quarks can change their distribution only through gluon bremsstrahlung. On the other hand, the Q^2 dependence of the sea is governed by two processes : gluon bremsstrahlung and pair creations. The coexistence of these two processes makes the Q^2 dependence of the sea very complicated. This is also clear from Eqs. (2.7)-(2.8). The Q^2 dependence of valence quarks is given for $0 \leq s \leq 1.2$ to a very good approximation by

$$x V(x,s) = \frac{3}{B(\alpha_1(s),\, 1+\alpha_2(s))}\, x^{\alpha_1(s)} (1-x)^{\alpha_2(s)} \qquad (3.5)$$

with

$$\alpha_1(s) = 0.65 - 1.15 \cdot G \cdot s \qquad (3.6)$$

$$\alpha_2(s) = 3 + 4.9 \cdot G \cdot s \qquad (3.7)$$

and

$$G = \frac{4}{(33 - 2m)}$$

Here $B(\ ,\ )$ is Euler's beta function. Notice that Eq. (3.5) satisfies the sum rule

$$\int dx\ V(x,s) = 3 \tag{3.8}$$

expressing the number of valence quarks in the nucleon. We have plotted $V(x,s)$ for various values of s in Fig. 1.

The Q^2 evolution of the sea depends on the shape of the gluon distribution, so we must consider various cases. We have taken η to be 3 and 9, the commonly believed limiting choices for the gluon distribution. The result for $S(x,s)$ is presented in Fig. 2. We do not present the corresponding distributions for $C(x,s)$ since the production off charmed quarks is still small at presently available energies and so we have not used them in our calculations of deep inelastic scattering *). $C(x,s)$ for various choices of gluon distribution can be found in Ref. 20).

We have checked that $V(x,s)$ and $S(x,s)$ as presented in Figs. 1 and 2 together with the corresponding $C(x,s)$ distribution reproduce quite well the μp data of Ref. 17). That they also are consistent with the data of Ref. 16) has been shown in Ref. 5).

In order to understand the results of Section 4 it is useful to recall a few basic properties of the Q^2 dependence of the quark distributions as given by ASFT.

With increasing Q^2 :

i) the momentum carried by valence quarks <u>decreases</u> and that carried by the sea <u>increases</u> ;

ii) the average value $\langle x \rangle$ <u>decreases</u> for both valence and sea quark distributions ;

---

*) Needless to say the charmed sea will manifest itself more visibly in electroproduction and μp deep inelastic scattering due to higher charge carried by charmed quarks relatively to d and λ quarks.

iii) both valence and sea quark distributions decrease at large x ;

iv) there is a strong (weak) increase of the sea (valence) distribution at small x.

The numerical estimates of i)-iii) are given in Table III. All those properties are clearly seen in Figs. 1 and 2.

4. - APPLICATION TO NEUTRINO AND ANTINEUTRINO PROCESSES

Having the Q^2 dependent quark densities at hand we shall calculate various cross-sections and distributions relevant for neutrino and antineutrino processes.

4.1. - General formulae for $d\sigma/dxdy$

We shall restrict ourselves to two weak interaction models, the GIM model and the five-quark model with a right-handed doublet $\binom{p}{b}_R$ [22]. We think it is still premature to discuss models with 8 or 10 flavours.

In calculating the charm of b quark production we shall utilize the modified scaling variable of Ref. 24) [see Eq. (4.5)]. On the other hand, we shall neglect target mass corrections as well as the mass corrections due to heavy quarks inside the nucleon. There are two reasons for this. First, it turns out [25] that target mass corrections are very small, much smaller than ASFT effects. Secondly we do not feel [25),26] justified in using the generalized scaling variable of Ref. 24) (with target and initial heavy quark masses included) before the importance of higher order corrections as well as of higher twist operators has been estimated in more detail. We hope to return to these questions in the future. On the other hand the effects of heavy quarks in the final state cannot be neglected since they lead to sizeable distortions of various distributions [27]. The formulae for $d\sigma/dxdy$ for the models under discussion have appeared already at many places in the literature [28]. We recall them nevertheless for completeness. We have, in units of G^2ME/π

$$\left(\frac{d\sigma}{dx\,dy}\right)^{\nu} = x\left\{ V(x,Q^2)\cos^2\theta_c + \frac{1}{3} S(x,Q^2)\left(1+(1-y)^2\right)\right\}$$

$$+ \xi_c\, y_c \left\{ V(\xi_c,Q^2)\sin^2\theta_c + \frac{1}{3} S(\xi_c,Q^2)\right\}\theta(1-\xi_c)$$

$$+ \xi_b\, y_b \frac{1}{3} S(\xi_b,Q^2)\,\theta(1-\xi_b) \qquad (4.1)$$

and

$$\left(\frac{d\sigma}{dx\,dy}\right)^{\bar{\nu}} = x\left\{ V(x,Q^2)(1-y)^2 + \frac{1}{3} S(x,Q^2)\left(1+(1-y)^2\right)\right\}$$

$$+ \xi_c\, y_c \frac{1}{3} S(\xi_c,Q^2)\,\theta(1-\xi_c)$$

$$+ \xi_b\, y_b \left\{ V(\xi_b,Q^2) + \frac{1}{3} S(\xi_b,Q^2)\right\}\theta(1-\xi_b) \qquad (4.2)$$

The first, second and third terms in Eqs. (4.1) and (4.2) refer to light quark production, charmed quark production and b quark production, respectively.

The variables entering Eqs. (4.1)-(4.2) are

$$x = \frac{Q^2}{2M\nu} \quad , \quad y = \frac{\nu}{E} \qquad (4.3)$$

$$y_a \equiv 1 - \frac{m_a^2}{2ME\xi_a} \qquad (4.4)$$

$$\xi_a = x + \frac{m_a^2}{2MEy} \qquad (4.5)$$

$$a = c, b$$

m_c and m_b are the masses of the charmed and bottom quarks, respectively.

In the numerical calculations we have used the values $m_c = 1.5$ GeV and $m_b = 5$ GeV.

Finally the range of variation of x and y (for $Q_o^2 \leq Q^2$) is,

i) for light quarks in the final state

$$\frac{Q_o^2}{2MEy} \leq x \leq 1 \quad , \quad \frac{Q_o^2}{2ME} \leq y \leq 1 \tag{4.6}$$

and

ii) for heavy quarks in the final state

$$\frac{Q_o^2}{2MEy} \leq x \leq 1 - \frac{m_a^2}{2MEy} \quad , \quad \frac{m_a^2 + Q_o^2}{2ME} \leq y \leq 1 \tag{4.7}$$

4.2. - Numerical estimates

The results which follow are based on Eqs. (4.1)-(4.7) and Q^2 dependent distributions obtained in Section 3.2. Since we have discussed many cases it is useful to introduce the following notations :

a) $\overline{\text{ASF}}$(ASF) - GIM model with asymptotic freedom effects included and with (without) cut-off at $Q_o^2 = 2$ GeV^2 ;

b) $\overline{\text{BASF}}$(BASF) - as a) but for the b quark model ;

c) $\overline{\text{FPM}}$(FPM) - as a) but without asymptotic freedom effects included, and

d) $\overline{\text{BFPM}}$(BFPM) - as c) but for the b quark model.

Since perturbation theory is bad for low Q^2 values, the calculations without Q^2 cut-off involved the assumption that all cross-sections for $Q^2 \leq 2$ GeV^2 are described by the free parton model. We again emphasize that we do not subscribe to such a procedure. Nevertheless we present such calculations for illustration and comparison with Q^2 cut results. Our results are presented in Figs. 3-7. It is easy to understand them on the basis of Eqs. (4.1)-(4.7) and our remarks at the end of Section 3.2. Therefore we only comment briefly on Figs. 3-7.

In Fig. 3a we have presented the ratio $R = (\sigma^{\bar{\nu}}/\sigma^{\nu})$ cut at $Q^2 = 2$ GeV^2 as a function of the incoming energy for the various cases mentioned above. The corresponding results without the cut-off in Q^2

are shown in Fig. 3b. Figure 3a also shows the dependence of R on the shape of the gluon distribution, which is weak. Notice that the dependence of R on E is much stronger in Fig. 3a. $\overline{\text{ASF}}$ and $\overline{\text{BASF}}$ give an increase in R of 40% and 100%, respectively, as we vary E from 30 to 150 GeV. The corresponding values for ASF and BASF are 10% and 65%. This difference is due both to the opening up of phase space [see Eqs. (4.6) and (4.7)] and the fact that the scaling part of the cross-section has been subtracted in Fig. 3a, leaving us with the pure asymptotic freedom effects. Notice also that whereas scaling violations lead to an enhanced increase of R in the GIM model relative to the free parton model predictions [2], they suppress slightly the corresponding increase in the b quark model. This is easy to understand if one recalls that in $\bar{\nu}(\nu)$ scattering b quark production occurs mainly off the valence quarks (sea) whereas charm production is off the sea (valence quarks and sea). The suppression of valence quarks and the increase of sea due to asymptotic freedom lead to the effects in question. We could conclude on the basis of Fig. 3b that ASF fails in describing the energy dependence of R, whereas the b quark model fits it rather well. But since the calculations of Fig. 3b were based on a doubtful assumption about the low Q^2 region (outside the field theoretical framework) we prefer to defer a final conclusion until we have data with a proper cut-off in Q^2, which we could compare with Fig. 3a.

The above discussion and comments also apply to Fig. 4 where we have plotted $\langle y \rangle_{\bar{\nu}}$ as function of E for the various cases considered. The decrease of $\langle y \rangle_{\bar{\nu}}$ with E for $\overline{\text{ASF}}$ and $\overline{\text{FPM}}$ is due to the opening of the phase space at small y values [see, e.g., Eqs. (4.6)-(4.7)], which cannot be compensated by asymptotic freedom effects. On the other hand, the increase of $\langle y \rangle$ with E due to appearance of heavy quarks with right-handed couplings is strong enough to win over the phase space effects in question. This very different behaviour of $\langle y \rangle_{\bar{\nu}}$ for $\overline{\text{ASF}}$ and $\overline{\text{BASF}}$ should be very helpful in distinction between models with right-handed and left-handed couplings.

Although $\langle y \rangle_{\bar{\nu}}$ as given by $\overline{\text{ASF}}$ decreases with E due to the phase space effects mentioned above, the theory in question predicts an increase of $(\pi/G^2ME)(d\sigma/dy)$ at large values of y. This is shown in Fig. 5. In Fig. 5a we have plotted $(\pi/G^2ME)(d\sigma/dy)$ at $E = 30$ GeV for $\overline{\text{FPM}}$ and $\overline{\text{ASF}}$ for two choices of gluon distribution. The distribution as given by $\overline{\text{ASF}}$ is flatter than that given by $\overline{\text{FPM}}$ because asymptotic freedom effects increase the importance of sea contributions, which have a flat y distribution.

The flattening out of $(\pi/G^2ME)(d\sigma/dy)$ at high values of y as given by ASFT depends only weakly on the shape of the gluon distribution. The effect in question is obviously stronger for broader gluon distribution.

In Fig. 5b the y distribution is shown for $\overline{\text{BASF}}$ and $\overline{\text{BFPM}}$ for two choices of gluon distribution and compared to the results of Fig. 5a. Only the $y \geq 0.5$ region has been shown since at $E = 30$ GeV only this part of the phase space is available for b quark production.

Figure 5c shows all the cases in question for $E = 150$ GeV. The distinction between various models is much clearer here than at $E = 30$ GeV.

In Fig. 6 we have shown the energy dependence of $\langle x \rangle$ for both ν and $\bar{\nu}$ processes for various cases considered. This decrease is due to both phase space and asymptotic freedom effects. The effect of pure asymptotic freedom can be inferred by comparing, for instance, the $\overline{\text{ASF}}$ curve with the $\overline{\text{FPM}}$ curve. Although we find x distributions to be a good place to look for asymptotic freedom effects they are less useful in distinguishing between models with left and right-handed couplings.

Finally, in Fig. 7 we have shown the rate of charm production in ν and $\bar{\nu}$ processes and the corresponding rate for bottom production in $\bar{\nu}$. Notice that asymptotic freedom manifests itself differently in the three cases considered. It strongly increases charm production in $\bar{\nu}$, decreases bottom production in $\bar{\nu}$ and increases only slightly charm production in ν scattering. The first two cases have already been discussed in connection with Fig. 3. The small increase of charm production in ν scattering relative to the increase in $\bar{\nu}$ scattering is due to the fact that in the former process charm is produced off both valence and sea quarks whereas in the latter process it is produced off the sea quarks only. The decrease of the valence quark distribution with increasing E as given by asymptotic freedom suppresses slightly in ν scattering otherwise strong increase of charm production due to the increased importance of sea quarks.

Another observation which can be made on the basis of Fig. 7 is the following. If right-handed currents are indeed present in Nature with the strength given by the b quark model, one should observe a strong increase of dilepton events with increasing E. The discussion of dimuon events is, however, outside the scope of this paper. We hope to come to

this in a future publication, where we also present a detailed discussion of heavy quark production as well as our evaluation of the Q^2 dependence of heavy quark distributions inside the nucleon.

5. - SUMMARY

In this paper we have discussed asymptotic freedom effects in neutrino and antineutrino processes in the context of two fashionable models of weak interactions. Some of the aspects presented here have already been discussed in the literature [2),3),5),7),20),21)]. In fact our work has been motivated by these papers. As we discussed in detail in the Introduction, we do not always agree with the way the asymptotic freedom effects have been compared to the data so far.

We emphasize once again the importance of the cut-off in Q^2. Although the data for $\langle y \rangle_{\bar{\nu}}$ and $\sigma^{\bar{\nu}}/\sigma^{\nu}$ resemble BASF predictions rather than those of GIM nevertheless, we think it is impossible to solve the high y anomaly controversy [2),3),5)-7)] before the properly cut data are compared to curves like those in Figs. 3 and 4. We have illustrated the effect of a cut-off in Q^2 on several examples (Section 4).

We have also shown that the shape of the gluon distribution does not affect strongly neutrino and antineutrino cross-sections as well as x and y distributions. The same conclusion has been reached by other authors in connection with electroproduction [1)] and Drell-Yan production [22)] calculations.

In our numerical estimates (Section 4) we have concentrated on the quantities in which asymptotic freedom and right-handed current effects are most clearly seen. So, for instance, we have not discussed $\langle y \rangle_{\nu}$ or $(d\sigma/dy)_{\nu}$ where these effects are small. We leave such an analysis for the future.

We end our paper by making a few comments on effects which we have neglected in our analysis.

The formulae (2.5)-(2.11) which we have used for the calculation of the Q^2 dependence of the parton distributions are true only up to the leading order in the effective coupling constant, higher orders being neglected. The formulae in question do not involve the higher twist contributions in the Wilson expansion and target mass effects either. All these three effects are presumably equally important and should be included together in a phenomenological analysis. Although a great deal of understanding of these effects has been gained over the last year [9),25),26)] we feel it is too early to include the effects in question in our analysis. In particular not all the corrections to the moment sum rules of order $\tilde{g}^2$ have been calculated in the literature. Neither are the effects of higher twist operators clearly understood. The belief is that these effects are mainly important for small Q^2 values and for $x \to 1$. By making a cut-off in Q^2 we eliminate many of these effects at small values of x. Since the quark distributions are anyway small at $x \to 1$ the effects in question will presumably not change drastically our estimates of global quantities such as $\sigma^{\bar{\nu}}/\sigma^{\nu}$ and $\langle y \rangle_{\nu}$. They may, however, lead to visible changes in the y and x distributions near the kinematical boundaries. It is very important to make in the future a quantitative analysis with all these effects included before we can decide whether asymptotic free gauge theories are capable of describing the deep inelastic data.

ACKNOWLEDGEMENTS

I am grateful to Mary K. Gaillard for many helpful discussions at all stages of this work and for a very careful reading of the manuscript. I also thank John Ellis for a critical reading of the manuscript. Special thanks are due to M.R. Pennington and A. Stergiou for advices related to the inversion programme. Finally I would like to thank my wife Gurli and my colleagues in the Theoretical Physics Division at CERN for encouragement, and Chris Llewellyn Smith for one very interesting discussion.

n	α_n	β_n	γ_+	γ_{AA}	γ_-	$\gamma_{\psi\psi}$
2	0.429	0.429	0.747	0.320	0.000	0.427
3	0.925	0.288	1.386	1.328	0.609	0.667
4	0.980	0.170	1.852	1.832	0.817	0.837
5	0.992	0.119	2.192	2.182	0.960	0.971

TABLE I - Values of parameters α_n, β_n, $\gamma_\pm$, γ_{AA}, $\gamma_{\psi\psi}$ entering Eqs. (2.5)-(2.11) for $n = 2,3,4,5$ and $m = 4$.

s	0	0.2	0.4	0.6	0.8	1.0	1.2
$\Lambda = 0.5$ $Q_o^2 = 2$	2	3.17	5.56	11.05	25.57	71.25	249
$\Lambda = 0.2$ $Q_o^2 = 2$	2	4.75	13.7	49.9	241.6	1661	17491

TABLE II - Values of Q^2 corresponding to $s = 0.2$, 0.4, 0.6 0.8, 1.0 and 1.2 for $Q_o^2 = 2$ GeV^2 and $\Lambda = 0.2$ and 0.5 GeV.

s		0	0.2	0.4	0.6	0.8	1.0	1.2
$xV(x,Q^2)$	%	42	38.5	35.4	32.5	30.0	27.4	25.1
	$<x>$	0.292	0.278	0.265	0.253	0.241	0.230	0.219
$xS(x,Q^2)$	%	8.7	10.3	11.8	13.2	14.5	15.8	17.0
	$<x>$	0.091	0.094 0.080	0.091 0.071	0.085 0.062	0.078 0.055	0.071 0.049	0.064 0.044

TABLE III - Momentum (%) and $<x>$ for the valence quarks and sea distributions as functions of Q^2. The upper and lower value in the last row corresponds to $xG(x,Q_o^2) \sim (1-x)^3$ and $xG(x,Q_o^2) \sim (1-x)^9$.

REFERENCES

1) G. Parisi and R. Petronzio - Phys.Letters 62B, 331 (1976).

2) G. Altarelli, R. Petronzio and G. Parisi - Phys.Letters 63B, 183 (1976) ;
G. Parisi - Proceedings of the Eleventh Rencontre de Moriond (1976).

3) R.M. Barnett, H. Georgi and H.D. Politzer - Phys.Rev.Letters 37, 1313 (1976).

4) M. Glück and E. Reya - Mainz Preprint MZ-TH-76-2 (1976).

5) M. Glück and E. Reya - Mainz Preprint MZ-TH-76-10 (1976).

6) K. Schilcher - Mainz Preprint MZ-TH-76-4 (1976).

7) V.A. Novikov et al. - ITEP Preprint 112 (1976).

8) P.W. Johnson and W.K. Tung - Illinois Institute of Technology Preprint (1976).

9) A. De Rujulà, H. Georgi and H.D. Politzer - Harvard Preprint, HUTP 76/A155 (1976).

10) V. Baluni and E. Eichten - Phys.Rev.Letters 37, 1181 (1976).

11) T. Kawaguchi and H. Nakkagawa - Kyoto University Preprint 76-16 (1976).

12) H.D. Politzer - Phys.Letters C14, 129 (1974).

13) D. Gross and F. Wilczek - Phys.Rev. D8, 3633 (1973) ; Phys.Rev. D9, 980 (1974) ;
H. Georgi and H.D. Politzer - Phys.Rev. D9, 416 (1974) ;
D. Balin, A. Love and D. Nanopoulos - Nuovo Cimento Letters 9, 501 (1974).

14) A. Benvenuti et al. - Preprint HPWF-76/2 (1976) ;
A. Benvenuti et al. - Phys.Rev.Letters 36, 1478 (1976) ; 37, 189 (1976).

15) B. Barish - Aachen Neutrino Conference (June 1976) and Caltech Preprint CALT 68-544 (1976).

16) C. Chang et al. - Phys.Rev.Letters 35, 901 (1975) ;
E.M. Riordan et al. - Phys.Rev.Letters 35, 901 (1975).

17) H. Anderson et al. - Contribution to the Tbilisi Conference 1976.

18) For a nice review, see : H. Fritzsch - CERN Preprint TH 2198 (1976) (Aachen Conference, 1976), and references therein.

19) B.W. Lee - Aachen Conference (1976).

20) I. Hinchliffe and C.H. Llewellyn Smith - Oxford Preprint 77 (1977).

21) A. Zee, F. Wilczek and S. Treiman - Phys.Rev. D10, 2881 (1974).

22) Y. Achiman, K. Koller and T.F. Walsh - Phys.Letters 59B, 261 (1975) ;
P. Fayet - Nuclear Phys. B78, 14 (1974) ;
R.M. Barnett - Phys.Rev. D13, 671 (1976) ;
F. Gürsey and P. Sikivie - Phys.Rev.Letters 36, 775 (1976) ;
P. Ramond - Caltech Preprint CALT 68-540 (1976).

23) V. Barger and R.J.N. Phillips - Nuclear Phys. B73, 269 (1974).

24) H. Georgi and H.D. Politzer - Phys.Rev.Letters 36, 1281 (1976), and Errata, Phys.Rev.Letters 37, 68 (1976).

25) G. Barbieri, J. Ellis, M.K. Gaillard and G.G. Ross - Phys.Letters 64B, 171 (1976), and Nuclear Phys. B117, 50 (1976).

26) D.J. Gross, S.B. Treiman and F.A. Wilczek - Princeton University Preprint (1976), and references therein.

27) R.M. Barnett - Phys.Rev.Letters 36, 1163 (1976).

28) J. Kaplan and F. Martin - Nuclear Phys. 115, 333 (1976) ;
C.H. Albright and R.E. Schrock - Fermilab Preprint 76/50 (1976) ;
V. Barger, R.J.N. Phillips and T. Weiler - Phys.Rev. D14, 1276 (1976).

FIGURE CAPTIONS

Figure 1 — Q^2 dependence of the valence quark distribution as given by asymptotic freedom. s is defined in Eqs. (2.12). See Table II for the corresponding Q^2 values.

Figure 2 — Q^2 dependence of the sea distribution a) $s = 0.4$, b) $s = 0.8$, for two shapes of the gluon distribution $(1-x)^3$ (upper solid line) and $(1-x)^9$ (dashed line). The lower solid line gives the sea at $s = 0$.

Figure 3 — Energy dependence of $\sigma^{\bar{\nu}}/\sigma^{\nu}$ for various cases discussed in the text. The lines (——) and (-•-•-) in Fig. 3a correspond to $xG(x,Q_o^2)$ equal to $(1-x)^3$ and $(1-x)^9$, respectively. The data in Fig. 3b are from Ref. 14) (circles) and Ref. 15) (squares).

Figure 4 — Energy dependence of $\langle y \rangle_{\bar{\nu}}$ for various cases discussed in the text. The data in Fig. 4b are from Ref. 14)

Figure 5 — $(\pi/MG^2E)(d\sigma/dy)_{\bar{\nu}}$ for various cases discussed in the text for $E = 30$ GeV [a) and b)] and $E = 150$ GeV [c)]. The meaning of lines (——) and (-•-•-) as in Fig. 3a.

Figure 6 — $\langle x \rangle_{\nu}$ and $\langle x \rangle_{\bar{\nu}}$ as functions of E for various cases discussed in the text.

Figure 7 — Charm and bottom production in various models discussed in the text.

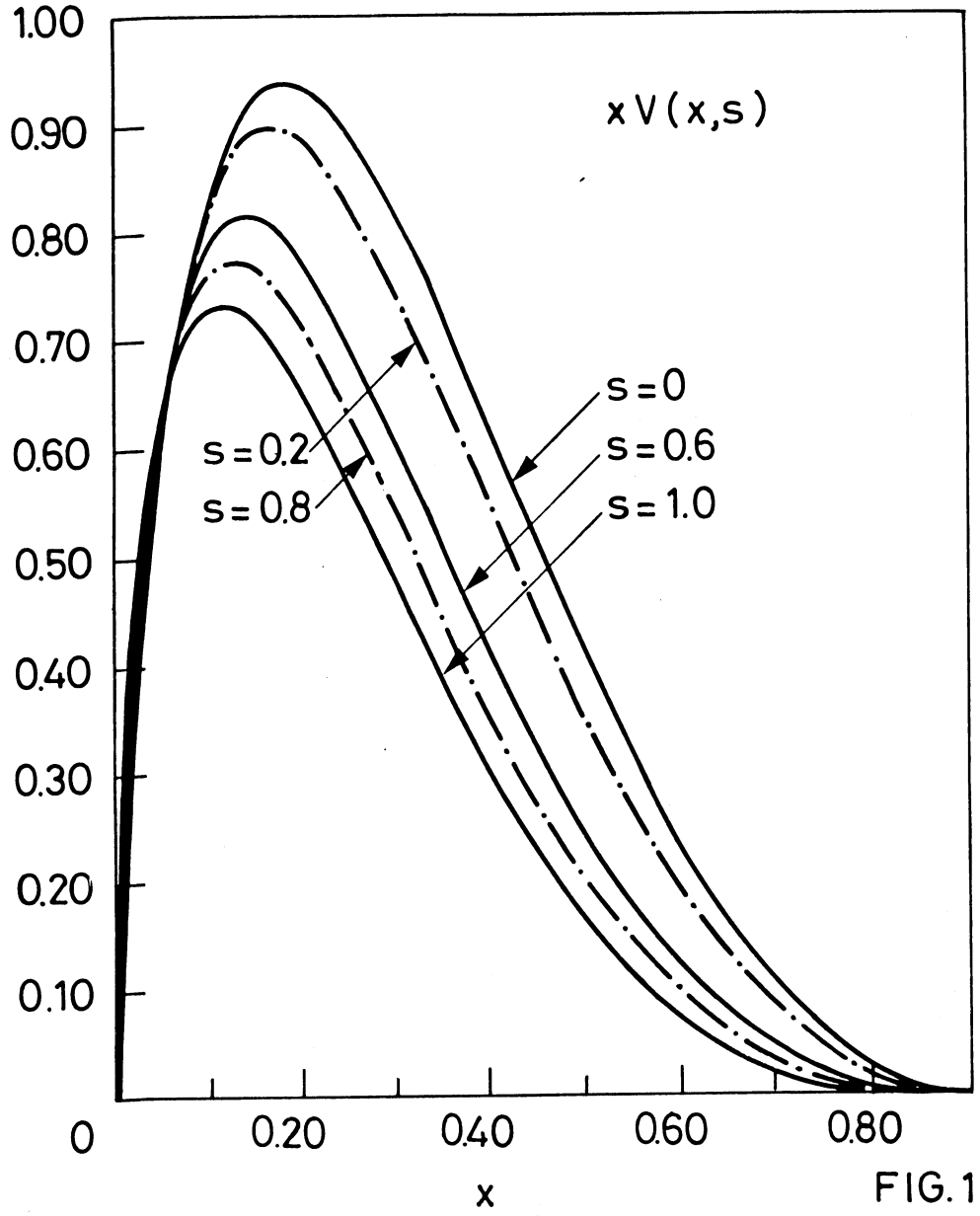
1.00
0.90
0.80
0.70
0.60
0.50
0.40
0.30
0.20
0.10
0
0.20
0.40
0.60
0.80
x
x V (x , s)
s = 0
s = 0.6
s = 1.0
s = 0.2
s = 0.8

FIG. 1

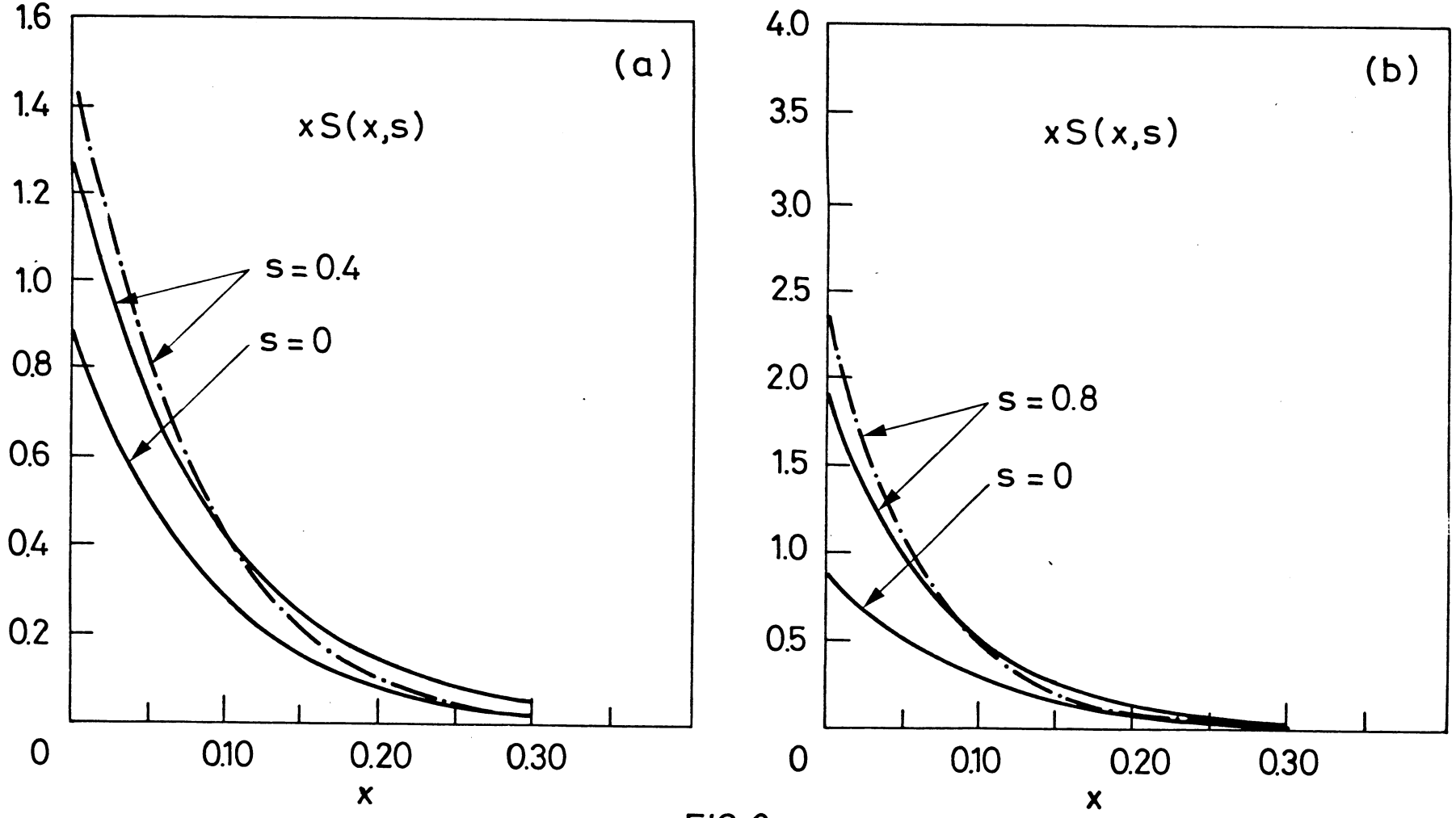
(a)
xS(x,s)
s = 0.4
s = 0
1.6
1.4
1.2
1.0
0.8
0.6
0.4
0.2
0
0.10
0.20
0.30
x
(b)
xS(x,s)
s = 0.8
s = 0
4.0
3.5
3.0
2.5
2.0
1.5
1.0
0.5
0
0.10
0.20
0.30
x

FIG. 2

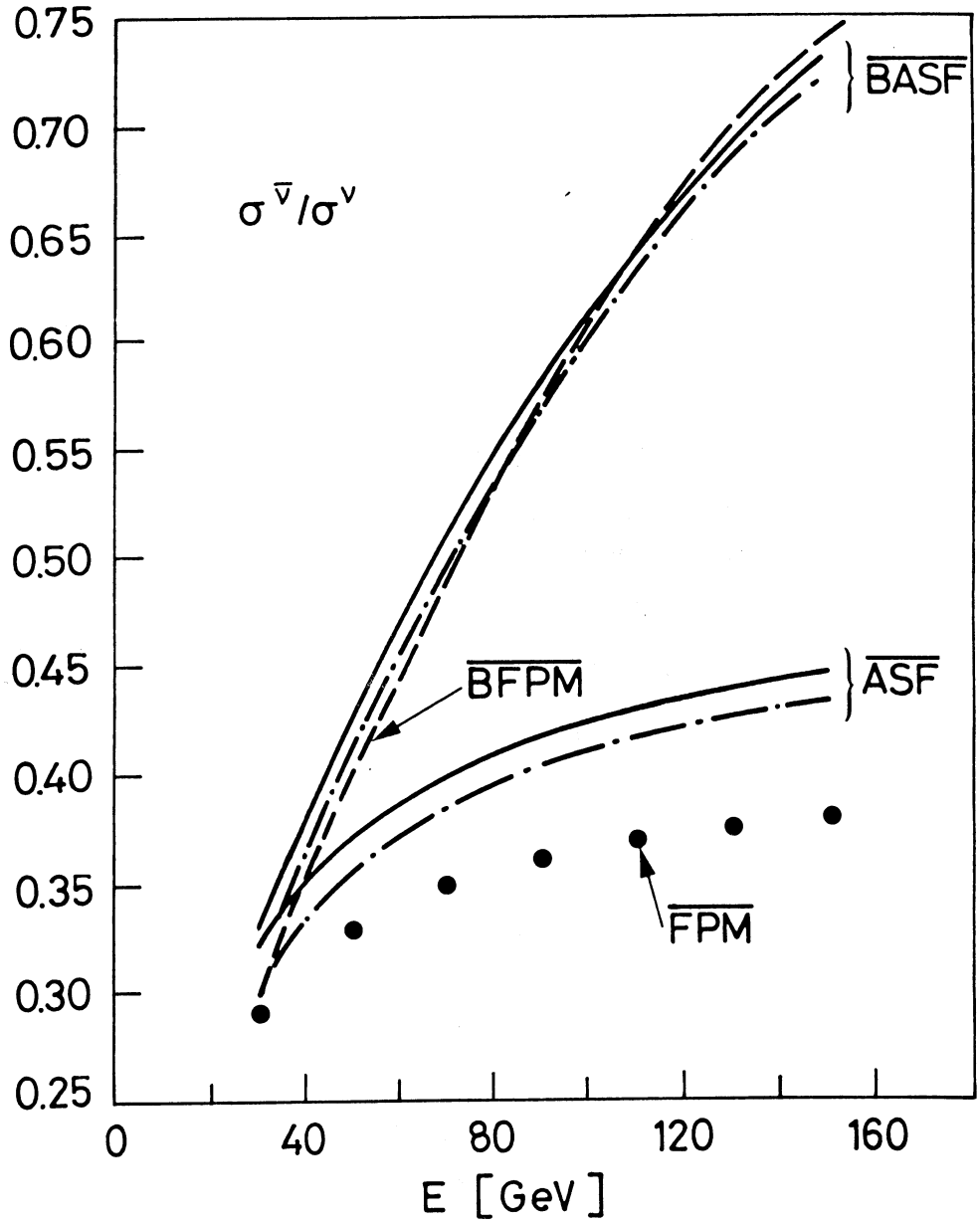
0.75
0.70
0.65
0.60
0.55
0.50
0.45
0.40
0.35
0.30
0.25
$\sigma^{\bar{\nu}}/\sigma^{\nu}$
$\overline{\text{BASF}}$
$\overline{\text{BFPM}}$
$\overline{\text{ASF}}$
$\overline{\text{FPM}}$
0
40
80
120
160
E [GeV]

FIG. 3a

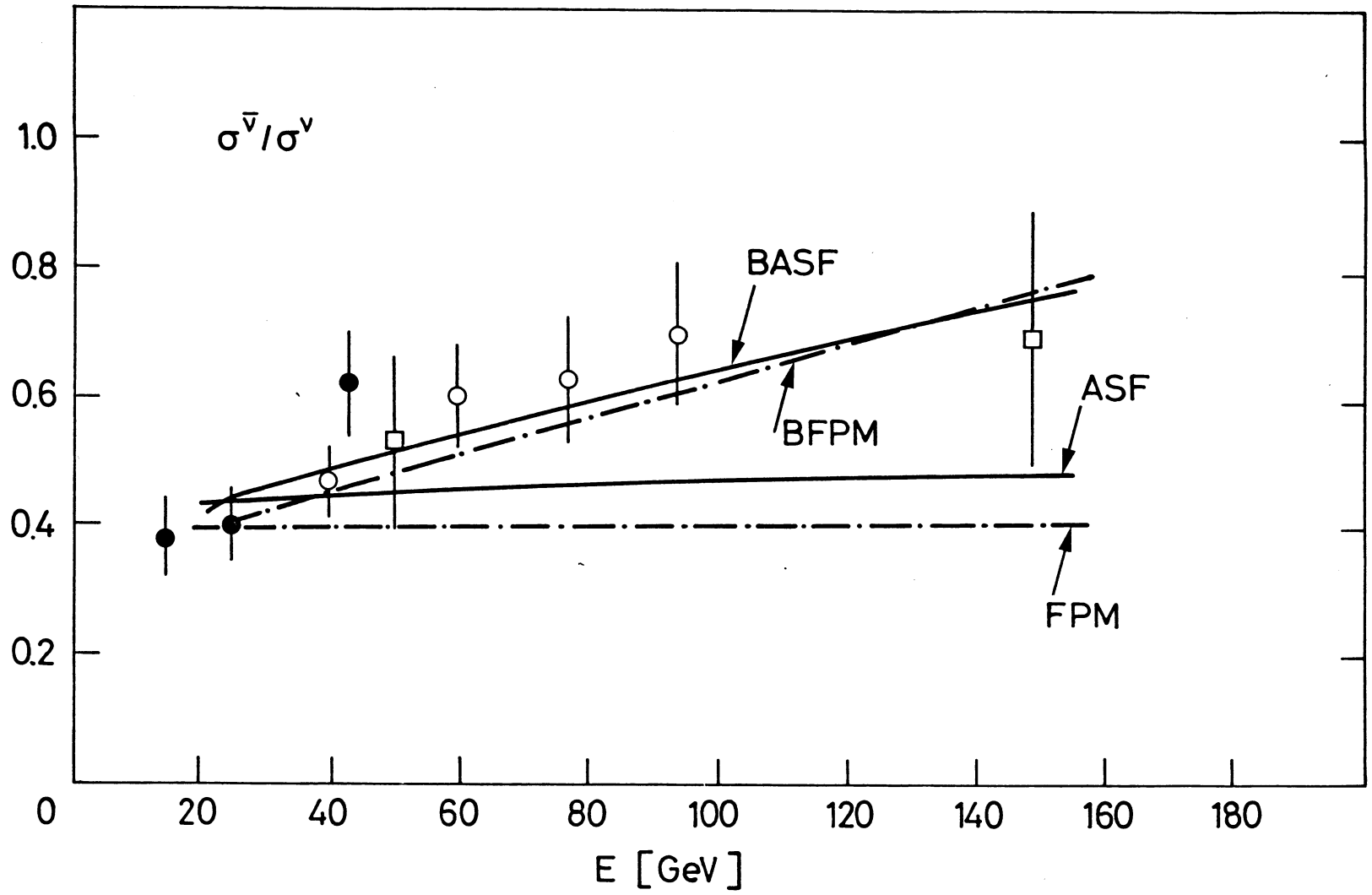
$\sigma^{\bar{\nu}}/\sigma^{\nu}$
1.0
0.8
0.6
0.4
0.2
0
20
40
60
80
100
120
140
160
180
E [GeV]
BASF
BFPM
ASF
FPM

FIG. 3 b

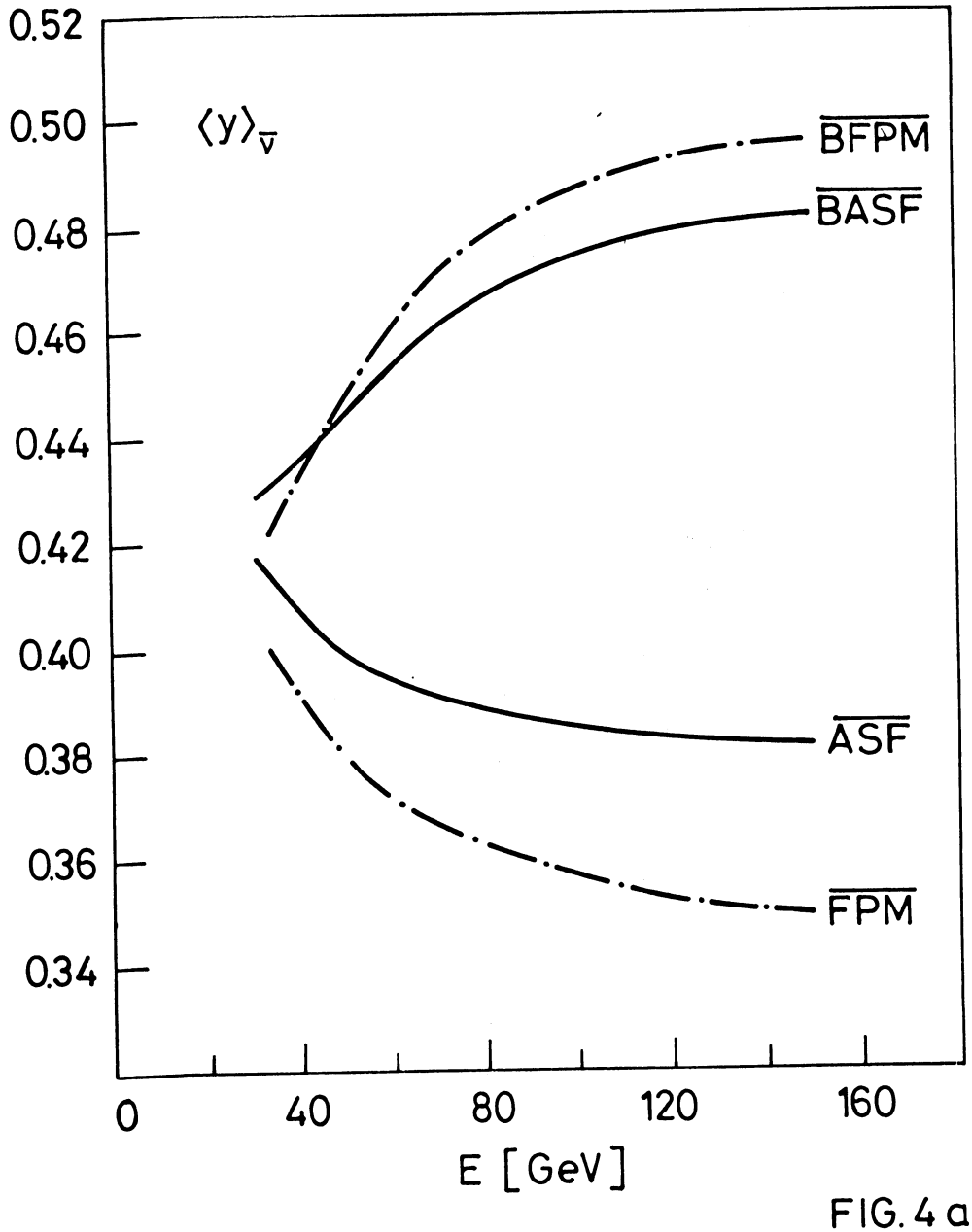
0.52
0.50
0.48
0.46
0.44
0.42
0.40
0.38
0.36
0.34
⟨y⟩$_{\bar{\nu}}$
$\overline{\text{BFPM}}$
$\overline{\text{BASF}}$
$\overline{\text{ASF}}$
$\overline{\text{FPM}}$
0
40
80
120
160
E [GeV]

FIG. 4 a

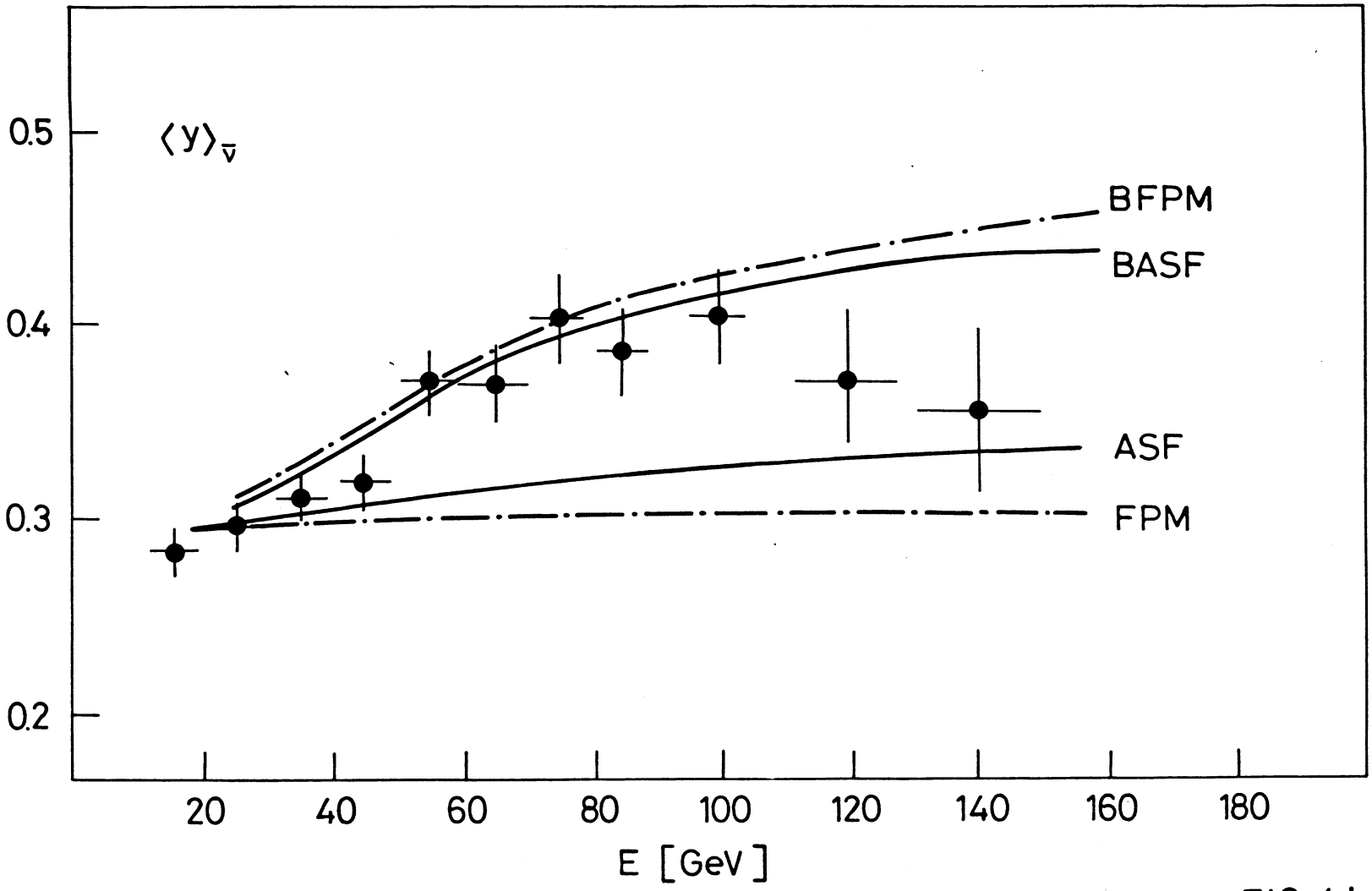
0.5
0.4
0.3
0.2
⟨y⟩ν̄
BFPM
BASF
ASF
FPM
20
40
60
80
100
120
140
160
180
E [GeV]

FIG. 4 b

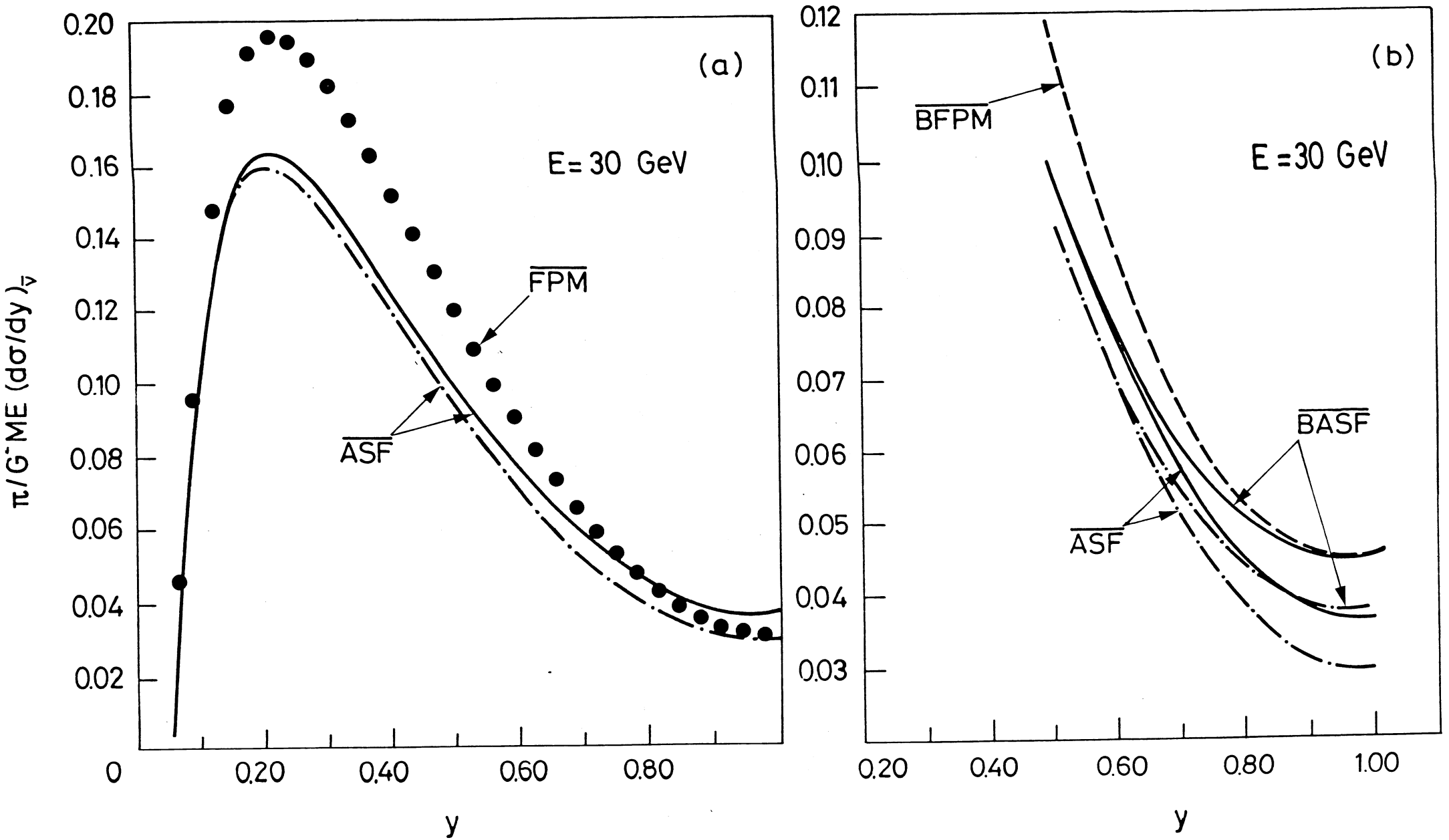
(a)
E= 30 GeV
FPM
ASF
π/G̃ME (dσ/dy)ν̄
y
0.20
0.18
0.16
0.14
0.12
0.10
0.08
0.06
0.04
0.02
0
0.20
0.40
0.60
0.80
(b)
E =30 GeV
BFPM
BASF
ASF
0.12
0.11
0.10
0.09
0.08
0.07
0.06
0.05
0.04
0.03
0.20
0.40
0.60
0.80
1.00

FIG. 5

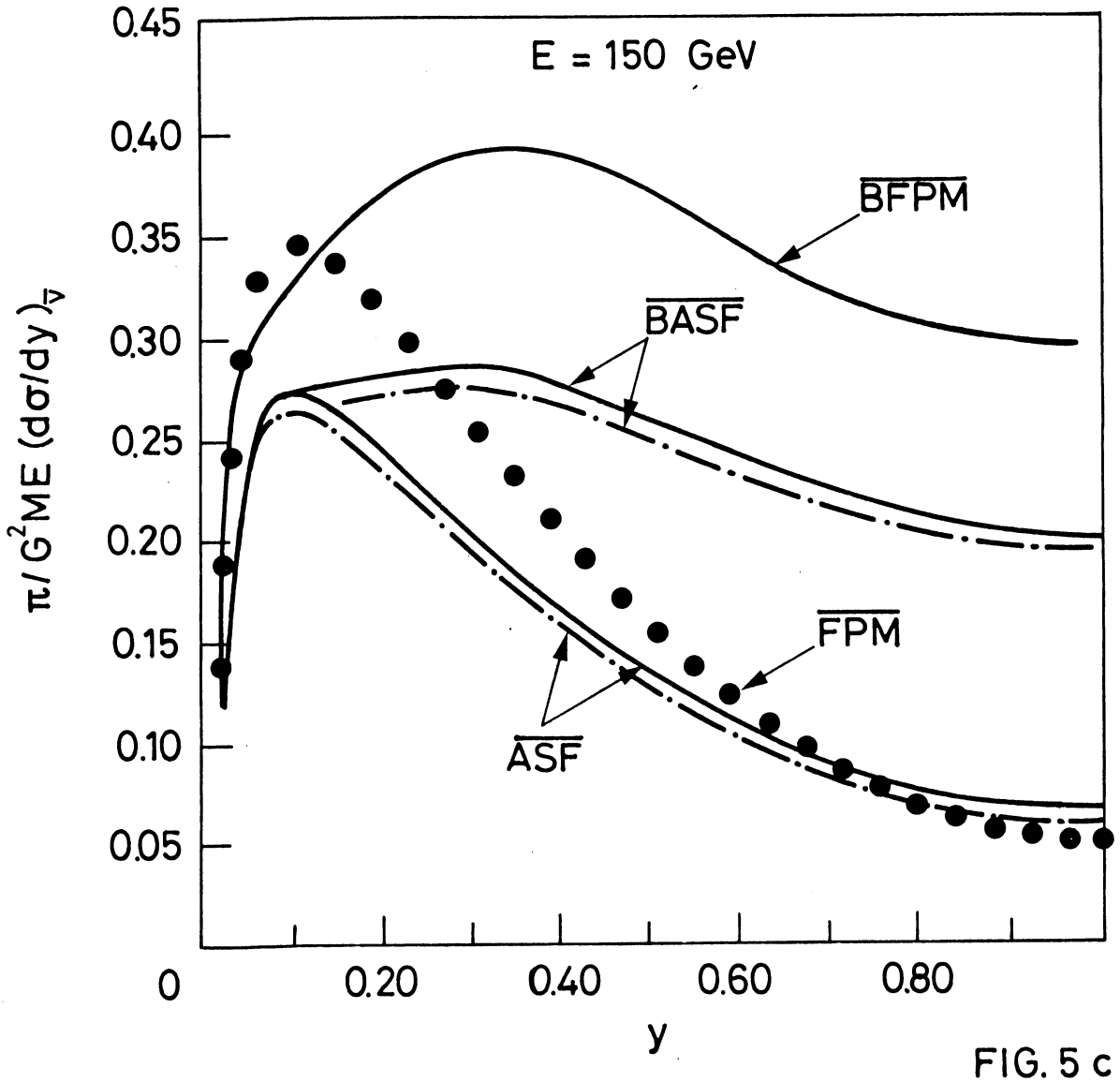
E = 150 GeV
$\overline{BFPM}$
$\overline{BASF}$
$\overline{FPM}$
$\overline{ASF}$
$\pi / G^2 ME \, (d\sigma/dy)_{\bar{\nu}}$
0.45
0.40
0.35
0.30
0.25
0.20
0.15
0.10
0.05
0
0.20
0.40
0.60
0.80
y

FIG. 5 c

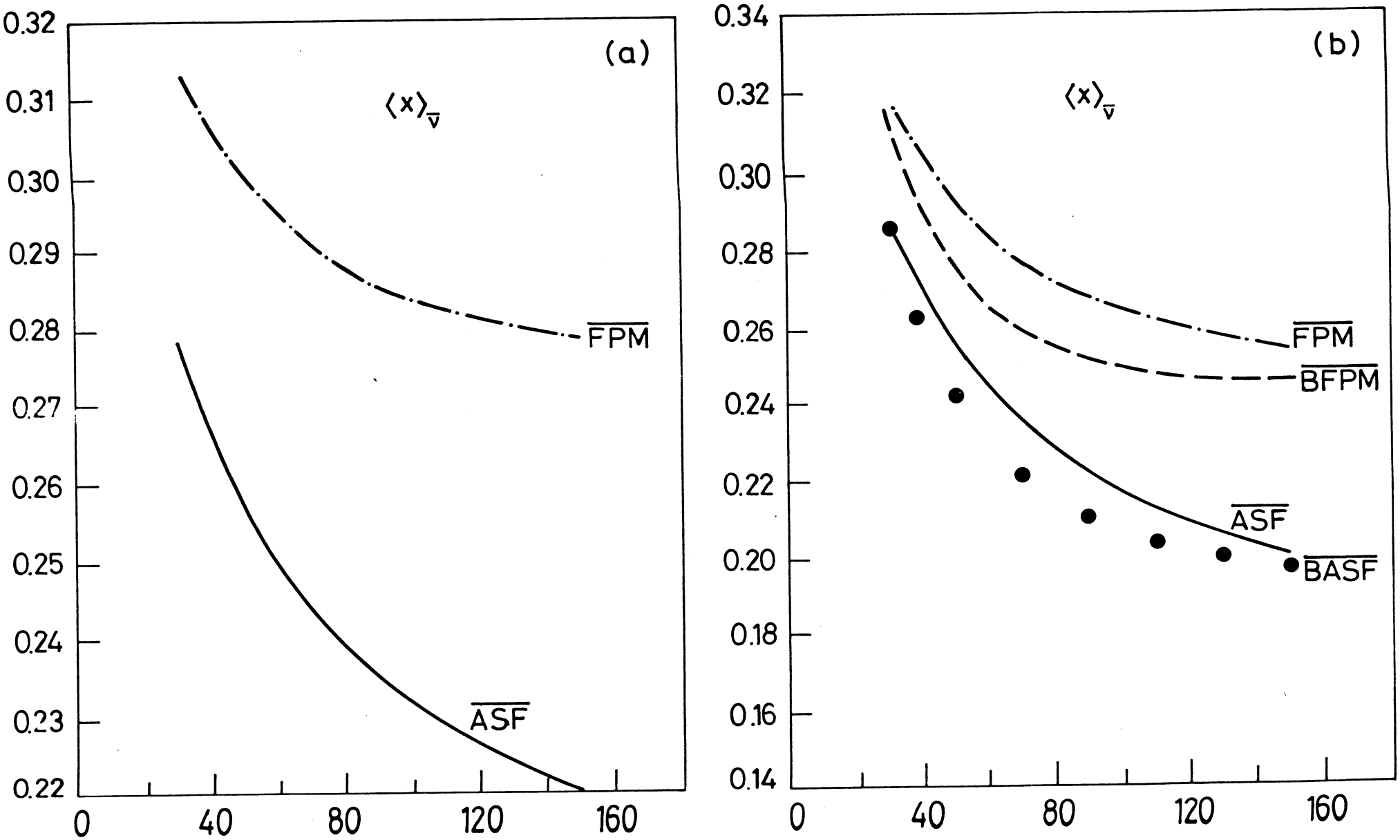
(a)
$\langle x \rangle_{\bar{\nu}}$
$\overline{FPM}$
$\overline{ASF}$
0.32
0.31
0.30
0.29
0.28
0.27
0.26
0.25
0.24
0.23
0.22
0
40
80
120
160
(b)
$\langle x \rangle_{\bar{\nu}}$
$\overline{FPM}$
$\overline{BFPM}$
$\overline{ASF}$
$\overline{BASF}$
0.34
0.32
0.30
0.28
0.26
0.24
0.22
0.20
0.18
0.16
0.14
0
40
80
120
160
E [GeV]

FIG.6

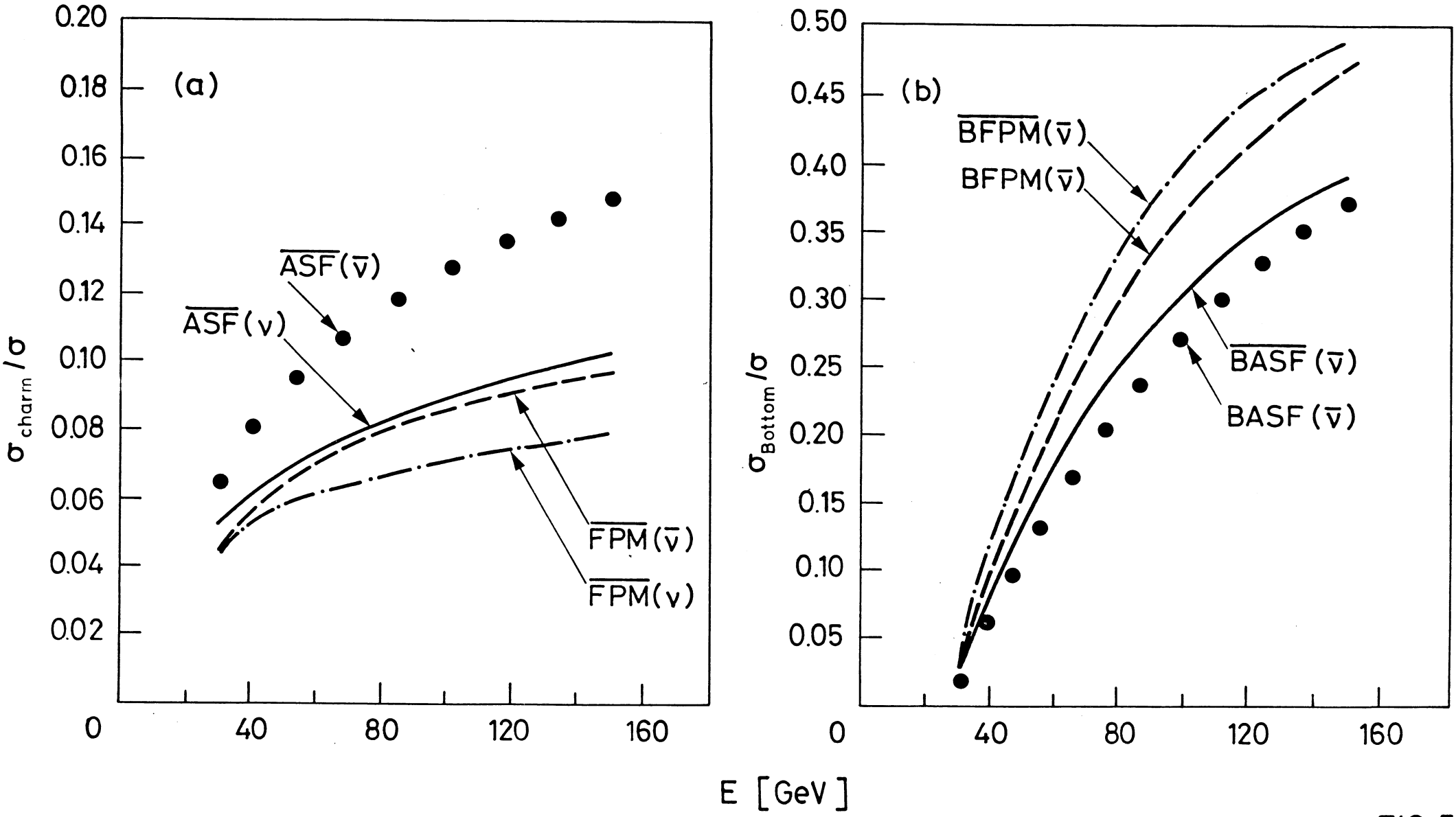
(a)
$\overline{ASF}(\bar{\nu})$
$\overline{ASF}(\nu)$
$\overline{FPM}(\bar{\nu})$
$\overline{FPM}(\nu)$
σ_{charm}/σ
0.20
0.18
0.16
0.14
0.12
0.10
0.08
0.06
0.04
0.02
0
40
80
120
160
(b)
$\overline{BFPM}(\bar{\nu})$
$BFPM(\bar{\nu})$
$\overline{BASF}(\bar{\nu})$
$BASF(\bar{\nu})$
σ_{Bottom}/σ
0.50
0.45
0.40
0.35
0.30
0.25
0.20
0.15
0.10
0.05
0
40
80
120
160
E [GeV]

FIG. 7